A Test Structure for in-situ Determination of Residual Stress

Akshdeep Sharma, Deepak Bansal, Kamaljit Rangra
Sensors and Nanotechnology Group
CSIR-Central Electronics Engineering Research Institute
(CEERI) Pilani Rajsthan India 333031
akshdeepsharma@gmail.com, kjrangra@gmail.com

Dinesh Kumar
Electronics Science Department
Kurukshetra University,Kurukshetra
Haryana, India 136119
dineshelctronics@gmail.com

***Abstract*— This work presents a lancet type residual stress measurement test structure which comprises of a pair of bent beams along with cantilevers as driving bars for the rotational pointer structure. The residual stress causes the bent beams to deflect each other, thereby magnifying the pointer deflection. The pointer deflection direction indicates the type of stress (compressive or tensile), with the displacement being independent of Young's modulus and film thickness. Finite element modeling is also used to analyze the structure and is compared with experimental results of electroplated Au structures.**

***Keywords—MEMS, residual stress,* test structure, FEM analysis**

I. INTRODUCTION

Residual stress measurement in thin films is a major concern related to the reliable operation of MEMS. Various methods have been published to extract the residual stress in polysilicon [1-3] and other materials such as SiO_2 and Si_xN_y [3]. Nowadays metallic film membranes e.g. Au, Ni are also being used in a range of MEMS applications [4, 5] such as RF MEMS. The robustness of thin metallic film is affected by compressive or tensile residual stress [6-9]. Measuring and controlling stress in these films is essential to ensure reliable microelectronic structures and microsytems.

II. TEST STRUCTURE

This paper reports study of residual stress in electroplated thin metallic film using lancet type structures [10] schematic of which are shown in figure 1 and 2. These structures consist of a pair of bent beams (tilted beams) with an apex cantilever (driving bar) at mid points and a rotational pointer. This structure has the advantage that it magnifies the pointer rotation by 10 times compared to other pointer test structures [5-9]. The magnifying pointer displacement gives the residual stress present in the material [11-13]. Lancet structures (symmetric and asymmetric) types have been fabricated as part of an RF MEMS switch fabrication [14]. Both types of structures are released by removing a sacrificial layer of photoresist in oxygen plasma. Figure 3 and 4 show a SEM micrograph of a resulting asymmetrical and symmetrical lancet structure. The interdigitated structures associated with the end of the pointer arms are designed to enable capacitance measurements caused by pointer deflection.

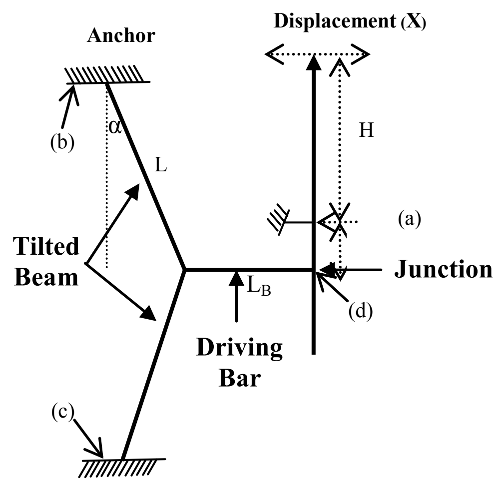

Figure 1 Conceptual schematic of the asymmetric lancet test structure.

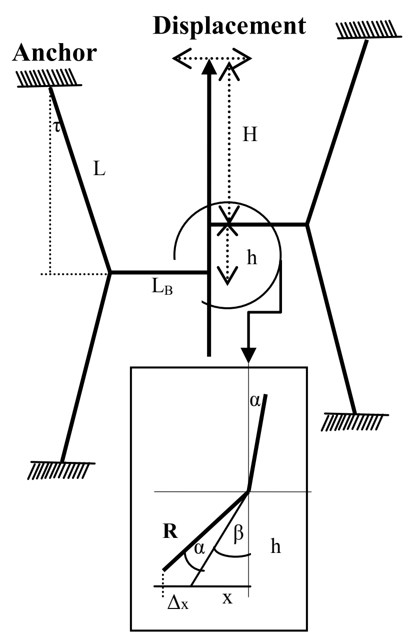

Figure 2 Conceptual schematic of the symmetric lancet with magnify image between anchor and junction

III. DESIGN OF THE TEST STRUCTURE

The important geometrical variables of the model are identified in figure 1. The following analytical model relates the planar strain of the structure with respect to the substrate, for a given displacement of the pointer. The lancet is fixed at point (a), with length (H) and distance (h) between the anchor (a) and the junction (d). The tilted arms are fixed at points (b) and (c), with length (L), inclination (α) and are connected with the lancet by a driving bar of length (L_B). When the structure is released, the residual stress induces strain in the tilted arms; this geometrical variation generates a force along the x-axis which leads to movement of the driving bar. The movement of the bar is amplified with respect to the tilted arm strain leading to the following relation between material strain and pointer displacement (X) for an asymmetric structure.

$$X = \frac{H}{h}\left\{\Delta L_B + (L+\Delta L)\,\mathrm{x}\sin\left[arccos\left(\frac{Lcos\alpha}{L+\Delta L}\right)\right] - Lsin\alpha\right\} \quad (1)$$

The symmetric lancet model is shown in figure 2. In this structure another tilted beam is added on the other side of asymmetric structure. It improves the robustness and helps the pointer to move in longitudinal direction. The displacement produced by strain of the material is magnified twice as compared to the earlier structure. As a consequence of the lancet thickness ($2x$), for this geometry a different model is required. The displacement Δx remains the same as for the asymmetric model. Total displacement in symmetrical model is: displacement = H sinα

$$= Hsin\left[\arcsin\left[\frac{x + \left\{\Delta L_B + (L+\Delta L) \times sin\left[arccos\left(\frac{Lcos\tau}{L+\Delta L}\right)\right] - Lsin\tau\right\}}{h/sin\beta}\right] - \beta\right] \quad (2)$$

The inclination (tilt angle α) plays an important role in defining the sensitivity of the structure. The structure efficiency (in terms of displacement) as a function of tilt angle α has been investigated using FEM simulation shown in figure 5. Figure 6 and 7 compare the displacement with residual strain calculated using the analytical model results for asymmetric and symmetric lancet. This shows reasonable agreement between the simulation and the analytical model with the FEM analysis consistently predicting larger displacements.

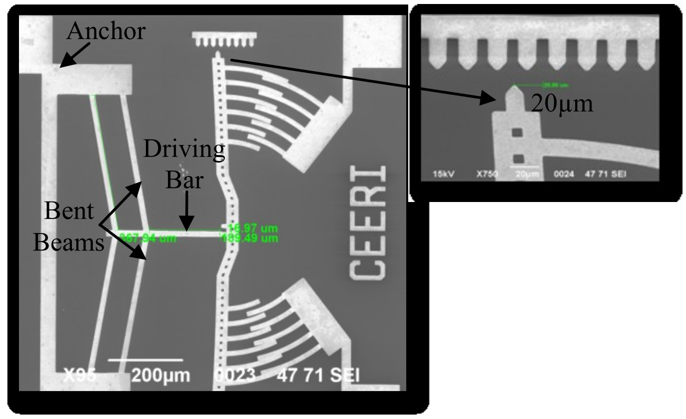

Figure 3. Asymmetrical rotational type lancet structure with pointer and vernier for measure displacement due to material strain

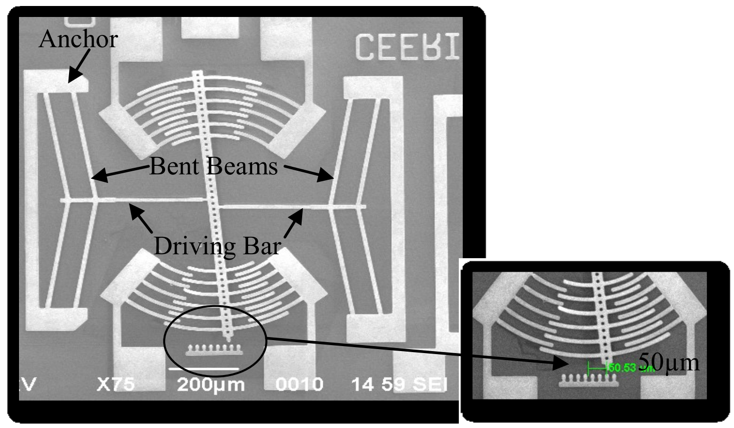

Figure 4. Symmetrical rotational type lancet structure with pointer and vernier for measure displacement due to material strain

IV. SIMULATION RESULTS

The finite element simulations were performed using COMSOL software [11], with a tilt angle of 10º,with material properties of gold from the MEMS material library (Young's modulus 70GPa, Poisson ratio 0.44, thermal expansion coeff. 14.2 x $10^{-6}K^{-1}$, thermal conductivity k=317W/mK, density ρ =19300kg/m^3, heat capacity at constant pressure C_p=129J/kgK). Simulation results of the displaced asymmetrical and symmetrical pointer are shown in figure 8 and 9. The structure was simulated for strains ranging from 0.0001 to 0.002, under an elastic regime. The maximum displacement and stress in asymmetrical lancet were 3.5µm and 221MPa, whereas in symmetrical lancet were 6.7 µm 226MPa respectively.

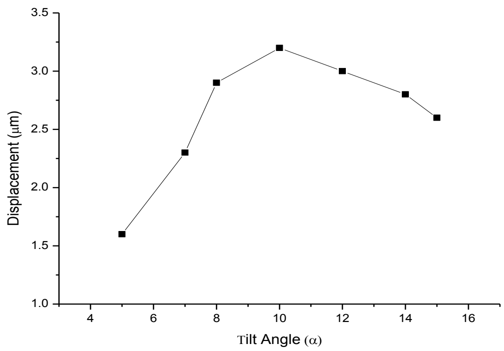

Figure 5 Simulated result of the displacement versus tilt angle

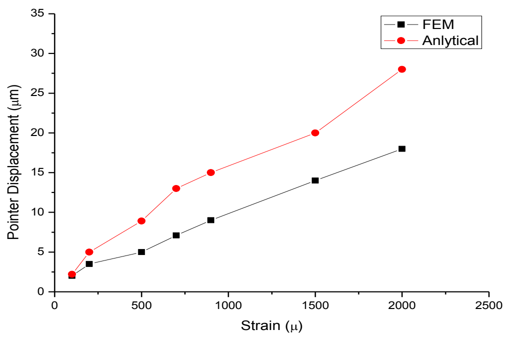

Figure 6 Pointer displacement as a function of residual strain both FEM and analytical models (Asymmetric Lancet)

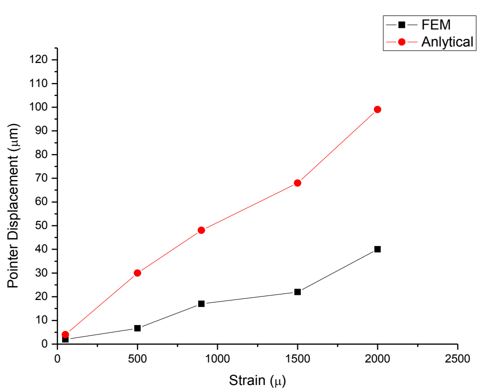

Figure 7 Pointer displacement as a function of residual strain both FEM and analytical models (Symmetric Lancet)

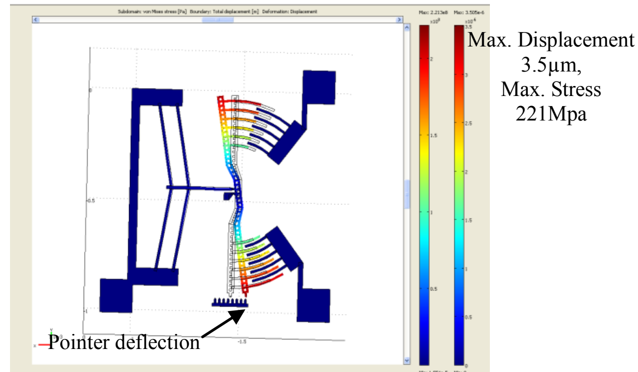

Figure 8 Simulated results of asymmetric lancet structure used to determine the maximum stress and displacement

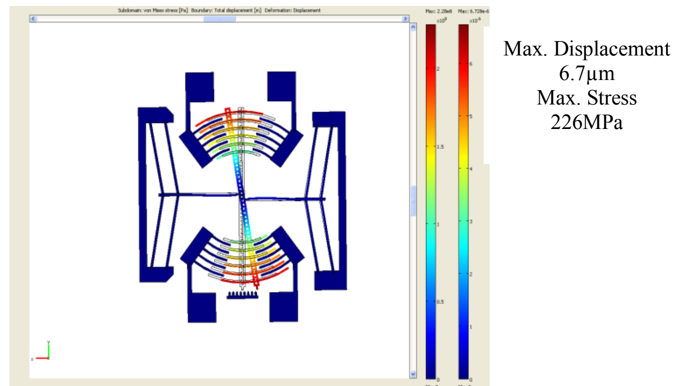

Figure 9 Simulated results of symmetric lancet structure used to determine the maximum stress and displacement

V. EXPERIMENTAL RESULTS

A SEM micrograph of a fabricated asymmetric and symmetric lancet structure is shown in figure 3 and 4. The pointer displacement was measured using SEM and also verified using an optical interferometer. As mentioned previously these structures were fabricated as part of a RF switch technology and significant variation in measured deflection were observed among similar structures on different wafers. A typical measured pointer deflection was 20μm and using the analytical expression the residual stress was calculated to be 200MPa, which indicates the resolution of structure, is 10MPa/μm. The observed pointer displacement in asymmetric structures varied 20-78μm whereas for symmetric structures this was 10-50μm. It is expected that there are spatial stress variations resulting from the electroplating process which has previously been reported for permalloy films [15]. Another source of stress variation may be related to the different ashing processes used during the release of MEMS structures.

VI. CONCLUSIONS

Simulations and in-situ stress measurements of electroplated gold asymmetric and symmetric lancet structures have been reported and the relative merits of the two structures are discussed. The symmetric pointer structure is a better choice due to maximum pointer displacement and less stress variation. A typical measured pointer deflection was 50µm and using the analytical expression the residual stress was calculated to be 226MPa, which indicates the resolution of structure is 5 MPa/µm.

ACKNOWLEDGMENT

Authors would like to acknowledge Director, CEERI, Pilani, for providing the design and fabrication facilities and CSIR New Delhi for financial support. The authors would also like to thank all the members of sensors and nanotechnology group for their help in fabrication of the devices.

REFERENCES

[1] M. Madou, Fundamentals of Microfabrication, CRC Press, USA, 1997.

[2] N.D. Masters, M.P. de Boer, B.D. Jensen, M.S. Baker, D. Koester, Side-by-side comparison of passive MEMS strain test structures under residual compression, in: C.L. Muhlstein, S.B. Brown (Eds.), Mechanical Properties of Structural Films, ASTM Special Technical Publication, vol. 1413, American Society for Testing and Materials, 2001, 1–33.

[3] J. Laconte et. al. F. Iker , S. Jorez , N. Andre, J. Proost , T. Pardoen, D. Flandre, J. P. Raskin , Thin films stress extraction using micromachined structures and wafer curvature measurements, Microelectronic Engineering 76 (2004), 219–226.

[4] S. Smith, N.L. Brockie, J. Murray, C.J. Wilson, A.B. Horsfall, J.G. Terry, J.T.M. Stevenson, A.R. Mount and A.J. Walton, Analysis of the Performance of a Micromechanical Test Structure to Measure Stress in Thick Electroplated Metal Films 2010 IEEE International Conference on Microelectronic Test Structures, March 22-25, Hiroshima, Japan

[5] J.G. Terry, S. Smith, A.J. Walton, A.M. Gundlach, J.T.M. Stevenson, A.B. Horsfall, K. Wang, J.M.M. dos Santos, S.M. Soare, N.G. Wright, A.G. O Neill, S.J. Bull, Test Chip for the Development and Evaluation of Test Structures for Measuring Stress in Metal Interconnect Proc. IEEE 2004 Int. Conference on Microelectronic Test Structures, 17 March 2004.

[6] B.P. van Drieenhuizen, J.F.L. Goosen, P.J. French, Comparison of techniques for measuring both compressive and tensile stress in thin films, Sens. Actuators A. 37/38 (1993) 756–765.

[7] L. Elbrecht, U. Storm, R. Catanescu, Comparison of stress measurement techniques in surface micromachining, J. Micromech. Microeng. 7 (1997) 151–154.

[8] B. Yogesh, K. Najafi, Gianchandani, Bent beam strain sensors, J. Microelectromech. Syst. 5 (1) (1996) 52–58.

[9] Q. He, Z.X. Luo, X.Y. Chen ,Comparison of residual stress measurement in thin films using surface micromachining method, Thin Solid Films 516, (2008) 5318–5323 .

[10] A. Bagolini, B. Margesin, A. Faes, G. Turco, F. Giacomozzi, Novel test structures for stress diagnosis in micromechanics, Sensors and Actuators A 115 (2004) 494-500.

[11] Akshdeep Sharma , Maninder Kaur, Dinesh Kumar and Kamaljit Rangra MEMS Test Structures for Residual Stress Measurement , COMSOL Conference 2010, Bangalore India 29 30 October 2010.

[12] Akshdeep Sharma, Deepak Bansal, Maninder Kaur, Prem Kumar, Dinesh Kumar and K. J. Rangra Fabrication and analysis of MEMS Test Structures for Residual Stress measurement , TechconnectWorld 2011 USA. NSTI ,accepted for Sensors and Transducer December 2011.

[13] Akshdeep Sharma, M. Kaur, D. Bansal, D. Kumar, K. Rangra, Review of mems test structures for mechanical parameter extraction, J. Nano-Electron. Phys. 3 (2011) No1, 243-253

[14] K. Rangra, "Electrostatic Low Actuation Voltage RF MEMS Switches for Telecommunications", Ph.D. Thesis, Department of Information Technology, University of Trento, Trento, Italy, 2005.

[15] J. Murray, G. Schiavone, S. Smith, N.L. Brockie, J.G. Terry, A.R. Mount, A.J. Walton; "Characterisation of Electroplated NiFe Films using Test Structures and Wafer Mapped Measurements", IEEE International Conference on Microelectronics Test Structures, 63-68, 4-7th April 2011.